The Astrophysical Journal, 1011:210 (8pp), 2026 November 10 https://doi.org/10.3847/1538-4357/aeaf53
© 2026. The Author(s). Published by the American Astronomical Society.
OPEN ACCESS

# Capturing Statistical Isotropy Violation with Rotational Averages

Vaishali R[1], Dipayan Mukherjee[1], Akshank Tyagi[1], and Tarun Souradeep[1,2]
[1] Raman Research Institute, C. V. Raman Avenue, Sadashivanagar, Bengaluru 560080, India; dipayan@rrimail.rri.res.in
[2] Inter University Centre for Astronomy and Astrophysics, Post Bag 4, Ganeshkhind, Pune-411007, India
*Received 2026 July 30; revised 2026 September 15; accepted 2026 September 29; published 2026 November 4*

## Abstract

Recent high-precision cosmological observations have revealed several anomalies in the cosmic microwave background (CMB), indicating possible violations of statistical isotropy (SI)—rotational invariance of statistical measures of a random skymap. The bipolar spherical harmonic (BipoSH) formalism, a widely used complete representation of both the SI and statistical anisotropy (nSI) components of a random skymap, is defined and implemented in the spherical harmonic space. In this work we probe the rotational symmetry violation of the correlation function using weighted rotational averages, providing a geometric interpretation of BipoSH as a real-space operation. We establish that the BipoSH measures are related to averages of the correlation function over all rotated configurations weighted by Wigner matrices. As a demonstration, we consider a phenomenological dipole modulation model and numerically implement the rotational average measures and show their agreement with their harmonic space counterparts. The real-space approach could be advantageous in formulating BipoSH like nSI measures on a partial sky. We envisage broader applications of this framework to the studies of primordial non-Gaussianity, CMB polarisation, weak gravitational lensing and the characterization of general random fields on a sphere.

*Unified Astronomy Thesaurus concepts:* Cosmology (343); Cosmic microwave background radiation (322); Cosmic anisotropy (316)

## 1. Introduction

The cosmological principle postulates that the Universe is homogeneous and isotropic on sufficiently large scales. Observations of the cosmic microwave background (CMB) and the large-scale structure support this ansatz, indicating a uniform Universe across hundreds of megaparsecs (K. K. S. Wu et al. 1999). Extended to cosmological perturbations, the principle requires the underlying stochastic field to be statistically homogeneous and isotropic, so that its correlation functions are invariant under spatial translations and rotations. For Gaussian fluctuations, this assumption collapses the entire statistical content of the CMB temperature anisotropies onto the angular power spectrum (Planck Collaboration 2020b).

As CMB observations have become increasingly precise, several features in the CMB sky, identified over the past two decades, suggest possible deviations from statistical isotropy (SI), collectively referred to as *CMB anomalies* (D. J. Schwarz et al. 2016; Planck Collaboration 2020a, 2020b). They could indicate a fundamental violation of homogeneity and isotropy in the physics of the early Universe (S. Prunet et al. 2005; C. Gordon 2007; S. M. Carroll et al. 2010; N. Bartolo et al. 2012; P. K. Rath et al. 2015; R. Kothari et al. 2016; P. K. Aluri et al. 2023; H. V. Ragavendra et al. 2025), or they may be artifacts of instrumental and observational systematics (S. Mitra et al. 2004; N. Joshi et al. 2010; S. Mukherjee & T. Souradeep 2014; S. Kumar et al. 2015; S. Das et al. 2016; Dipanshu et al. 2023). It is therefore imperative to systematically quantify statistical anisotropy (nSI) in CMB, both to discern its origin and to identify possible signatures of nontrivial physics in the very early Universe.

Original content from this work may be used under the terms of the Creative Commons Attribution 4.0 licence. Any further distribution of this work must maintain attribution to the author(s) and the title of the work, journal citation and DOI.

Quantifying general nSI in CMB is nontrivial for several key reasons. The CMB correlation functions are defined on the sphere and thus require a harmonic decomposition adapted to the spherical geometry—less straightforward than its three-dimensional Euclidean counterpart. Further, for a Gaussian field, SI imposes a unique structure on the correlation functions while its violation does not: isotropy can be broken in infinitely many ways (D. A. Varshalovich et al. 1988; A. Hajian & T. Souradeep 2003). Consequently, extracting a physical notion of the 'degree of anisotropy' remains challenging. Finally, CMB observations provide but a single realization of the underlying random process, a fundamental obstacle to statistical inference.

The standard route to a fully general treatment of CMB nSI is the bipolar spherical harmonic (BipoSH) basis (D. A. Varshalovich et al. 1988; A. Hajian & T. Souradeep 2003, 2005), which recasts anisotropy in the two-point function using the language of angular momentum addition. The multipole structures of the two line-of-sight directions are coupled into a state of total angular momentum $L$, with $L = 0$ recovering the usual power spectrum and $L > 0$ encoding nSI.

In this paper we introduce a complementary real-space framework. Because the $N$-point correlation functions are rotationally invariant under the hypothesis of SI, the natural real-space diagnostic is the average of the correlation function over all rotated configurations. The key ingredient is the choice of weight: by weighting this rotational average with Wigner matrices, we systematically isolate the nSI features at each bipolar $L$. We then map these rotational averages onto the BipoSH coefficients. This serves two ends. First, it endows the BipoSH formalism with a transparent, real-space geometric interpretation of how it encodes nSI. Second, it provides a new framework of extracting nSI signatures directly from real-space temperature data. We further extend the construction to the angular three-point correlation function in the Appendix.

The real-space approach carries advantages: it isolates the nSI signal at a given multipole without the full machinery of harmonic-space decomposition. Moreover, operating natively in real space sidesteps the partial sky artifacts—mode coupling and leakage—that inevitably afflict harmonic analysis of the masked CMB sky.

## 2. BipoSH Expansion

A general two-point function $C(\hat{\boldsymbol{n}}_1, \hat{\boldsymbol{n}}_2)$ is suitably expanded in the BipoSH basis, which couples the two internal ranks $(\ell_1, \ell_2)$ corresponding to the two directions $(\hat{\boldsymbol{n}}_1, \hat{\boldsymbol{n}}_2)$ into a state of total angular momentum $L$ (D. A. Varshalovich et al. (1988))

$$C(\hat{\boldsymbol{n}}_1, \hat{\boldsymbol{n}}_2) = \sum_{LM} \sum_{\ell_1\ell_2} A^{LM}_{\ell_1\ell_2} \mathbb{Y}^{LM}_{\ell_1\ell_2}(\hat{\boldsymbol{n}}_1, \hat{\boldsymbol{n}}_2), \tag{1}$$

where $A^{LM}_{\ell_1\ell_2}$ are the BipoSH coefficients; the BipoSH basis functions $\mathbb{Y}^{LM}_{\ell_1\ell_2}(\hat{\boldsymbol{n}}_1, \hat{\boldsymbol{n}}_2)$ are defined in terms of tensor product of two spherical harmonics

$$\begin{aligned}\mathbb{Y}^{LM}_{\ell_1\ell_2}(\hat{\boldsymbol{n}}_1, \hat{\boldsymbol{n}}_2) &\equiv \{Y_{\ell_1}(\hat{\boldsymbol{n}}_1) \otimes \ Y_{\ell_2}(\hat{\boldsymbol{n}}_2)\}_{LM} \\ &= \sum_{m_1 m_2} \mathcal{C}^{LM}_{\ell_1 m_1 \ell_2 m_2} Y_{\ell_1 m_1}(\hat{\boldsymbol{n}}_1) Y_{\ell_2 m_2}(\hat{\boldsymbol{n}}_2),\end{aligned} \tag{2}$$

where $\mathcal{C}^{LM}_{\ell_1 m_1 \ell_2 m_2}$ are the Clebsch–Gordan coefficients. The triangle inequality $|\ell_1 - \ell_2| \leqslant L \leqslant \ell_1 + \ell_2$ and the condition $M = m_1 + m_2$ are assumed in this expansion.

The coefficients $A^{LM}_{\ell_1\ell_2}$ fully encode the statistics of the two-point function in the harmonic space. For a Gaussian field they therefore encode the full statistical content of the field, whereas for a non-Gaussian field the higher-point functions carry independent information.

However, the nSI information is often spectrally spread out in the harmonic and bipolar–harmonic multipole space. Typically, one looks for nSI features in the correlation function at a given scale, characterized by the total multipole $L > 0$. Consequently, capturing the nSI signal for even a small $L$ mode (large scale) requires evaluating these coefficients up to arbitrarily high internal ranks. Most importantly, although mathematically robust, the abstract concept of angular momentum coupling obscures the geometric nature of the field wherein the underlying symmetry is broken in the case of nSI. We address this by presenting a real-space framework, specifically in the context of CMB temperature anisotropies.

## 3. Rotational Averages of Correlation Functions

Let $C(\hat{\boldsymbol{n}}_1, \hat{\boldsymbol{n}}_2,\ldots,\hat{\boldsymbol{n}}_N)$ be an arbitrary $N$-point function on $S^2 \times \cdots \times S^2$, where $\hat{\boldsymbol{n}}_i$ are unit vectors on a sphere. The function is isotropic if it is invariant under arbitrary rotations of its arguments

$$C(\hat{\boldsymbol{n}}_1, \hat{\boldsymbol{n}}_2,\ldots,\hat{\boldsymbol{n}}_N) = C(\mathrm{R}\hat{\boldsymbol{n}}_1, \mathrm{R}\hat{\boldsymbol{n}}_2,\ldots,\mathrm{R}\hat{\boldsymbol{n}}_N), \tag{3}$$

for all $\mathrm{R} \in SO(3)$. We define the average of $C$ over all rotated configurations as

$$\begin{aligned}I(\hat{\boldsymbol{n}}_1, \hat{\boldsymbol{n}}_2,\ldots,\hat{\boldsymbol{n}}_N) = \int_{SO(3)} \mathrm{d}\mu(\mathrm{R})\, W(\mathrm{R}) \\ \times C(\mathrm{R}\hat{\boldsymbol{n}}_1, \mathrm{R}\hat{\boldsymbol{n}}_2,\ldots,\mathrm{R}\hat{\boldsymbol{n}}_N),\end{aligned} \tag{4}$$

where $W(\mathrm{R})$ is a chosen rotation-dependent weight, and $d\mu(\mathrm{R})$ is the normalized Haar measure for the integration over the the rotation group $SO(3)$ (D. A. Varshalovich et al. 1988). If $C$ is isotropic, $I$ becomes proportional to $C$. For an nSI $C$, its rotated configurations differ, and the weighted average probes the sensitivity of $C$ to rotations thus providing a measure of the "degree of anisotropy" in $C$, where the choice of $W(\mathrm{R})$ determines how this information is extracted.

To arrive at suitable weight functions, it is instructive to consider the harmonic representations of these correlation functions. A generic one-point function $f(\hat{\boldsymbol{n}})$ is expanded in the standard spherical harmonic basis, $f(\hat{\boldsymbol{n}}) = \sum_{\ell m} f_{\ell m} Y_{\ell m}(\hat{\boldsymbol{n}})$, while the harmonic expansion of a general two-point function is given in the BipoSH basis in Equation (1). Importantly, a spatial rotation $\mathrm{R} \in SO(3)$ transforms these harmonic bases linearly via the Wigner-$D$ matrices (D. A. Varshalovich et al. (1988)), i.e., the spherical harmonics of multipole $\ell$ transforms as

$$Y_{\ell m}(\mathrm{R}\hat{\boldsymbol{n}}) = \sum_{m}{}' D^{\ell}_{m'm}(\mathrm{R}) Y_{\ell m'}(\hat{\boldsymbol{n}}), \tag{5}$$

whereas the BipoSH basis state of total angular momentum $L$ transforms analogously

$$\mathbb{Y}^{LM}_{\ell_1\ell_2}(\mathrm{R}\hat{\boldsymbol{n}}_1, \mathrm{R}\hat{\boldsymbol{n}}_2) = \sum_{M}{}' D^{L}_{M'M}(\mathrm{R}) \mathbb{Y}^{LM'}_{\ell_1\ell_2}(\hat{\boldsymbol{n}}_1, \hat{\boldsymbol{n}}_2). \tag{6}$$

It is important to note that the Wigner-D matrix mixes the azimuthal indices $M$, while preserving the angular structure indicated by $L$. Thus if a two-point function contains an $L$-th nSI correlation, its behavior under rotations is entirely dictated by the Wigner matrix. Therefore, a nonzero integral with a weight constructed from $D^{L}_{MM'}(\mathrm{R})$ would indicate the presence of symmetry violation in the correlation function at the $L$-th scale. Note that these matrices are orthogonal with respect to the normalized integration measure $d\mu(\mathrm{R})$ over $SO(3)$ (D. A. Varshalovich et al. 1988)

$$\begin{aligned}\int d\mu(\mathrm{R}) D^{L_1}_{M_1M_1'}(\mathrm{R}) D^{L_2*}_{M_2M_2'}(\mathrm{R}) = \frac{1}{2L_1+1} \\ \times \delta_{L_1L_2}\delta_{M_1M_2}\delta_{M_1'M_2'}.\end{aligned} \tag{7}$$

With this motivation, we now construct the weighted rotational averages for the CMB two-point correlation function.

### 3.1. Rotational Averages of CMB Two-point Correlation Function

In the following, we denote $C(\hat{\boldsymbol{n}}_1, \hat{\boldsymbol{n}}_2) = \langle \Delta T(\hat{\boldsymbol{n}}_1) \Delta T(\hat{\boldsymbol{n}}_2) \rangle$ to be the CMB correlation function, although the arguments shall remain valid for arbitrary two-point functions. In general, $C(\hat{\boldsymbol{n}}_1, \hat{\boldsymbol{n}}_2)$ is a real function defined on $S^2 \times S^2$. We now consider different weight functions based on Wigner matrices to extract nSI information of the correlation functions at varying levels of detail.

#### 3.1.1. Uniform Weight

If we choose the weight $W$ to be isotropic ($\propto D^0_{00}$), i.e., independent of rotations, then the correlation function is uniformly averaged over all rotations. In this case, $I(\hat{\boldsymbol{n}}_1, \hat{\boldsymbol{n}}_2)$ captures the *SI part* of the correlation function through real space (I. Szapudi et al. 2001). That is, setting $W(\mathrm{R}) = 1$

$$I(\hat{\boldsymbol{n}}_1, \hat{\boldsymbol{n}}_2) = I_{\mathrm{uni}}(\hat{\boldsymbol{n}}_1 \cdot \hat{\boldsymbol{n}}_2) \tag{8}$$

$$= \int d\mu(\mathrm{R}) C(\mathrm{R}\hat{\boldsymbol{n}}_1, \mathrm{R}\hat{\boldsymbol{n}}_2) \tag{9}$$

$$=\sum_{\ell}(-1)^{\ell}\frac{\sqrt{2\ell+1}}{4\pi}A^{00}_{\ell\ell}P_{\ell}(\cos\theta). \tag{10}$$

$I_{\rm uni}(\hat{\boldsymbol{n}}_1\cdot\hat{\boldsymbol{n}}_2)$ is a function of the relative angle $\theta=\cos^{-1}(\hat{\boldsymbol{n}}_1\cdot\hat{\boldsymbol{n}}_2)$ and $A^{00}_{\ell\ell}$ are the BipoSH coefficients. The coefficient in the Legendre expansion can be identified with the angular power spectrum $C_\ell$ as

$$A^{00}_{\ell\ell}=(-1)^{\ell}\sqrt{2\ell+1}\,C_{\ell}. \tag{11}$$

It is evident from above that the uniform rotational average is simply the isotropic angular correlation function

$$\begin{aligned}I_{\rm uni}(\hat{\boldsymbol{n}}_1\cdot\hat{\boldsymbol{n}}_2)&=\sum_{\ell}\frac{2\ell+1}{4\pi}C_{\ell}P_{\ell}(\cos\theta)\\&=C(\cos\theta).\end{aligned} \tag{12}$$

#### 3.1.2. Character Function as Weight

To extract information of nSI in $C(\hat{\boldsymbol{n}}_1,\hat{\boldsymbol{n}}_2)$ *at the multipole level*, we use the character function of the rotation group (D. A. Varshalovich et al. 1988)

$$\chi^{L}(\mathrm{R})=\sum_{M=-L}^{L}D^{L}_{MM}(\mathrm{R}) \tag{13}$$

as the weight in the rotational average, i.e.,

$$I^{L}(\hat{\boldsymbol{n}}_1,\hat{\boldsymbol{n}}_2)=\int d\mu(\mathrm{R})\,\chi^{L}(\mathrm{R})\,C(\mathrm{R}\hat{\boldsymbol{n}}_1,\mathrm{R}\hat{\boldsymbol{n}}_2). \tag{14}$$

The quantity $I^{L}(\hat{\boldsymbol{n}}_1,\hat{\boldsymbol{n}}_2)$ captures the violation of isotropy by the two-point correlation function at the $L$th multipole corresponding to the line-of-sight directions $\hat{\boldsymbol{n}}_1$ and $\hat{\boldsymbol{n}}_2$. We can further average the squared absolute quantity $|I^{L}(\hat{\boldsymbol{n}}_1,\hat{\boldsymbol{n}}_2)|^2$ over both the directions to arrive at a positive definite global measure of anisotropy

$$\kappa^{L}\equiv\int\frac{d\Omega_{\hat{\boldsymbol{n}}_2}}{4\pi}\int\frac{d\Omega_{\hat{\boldsymbol{n}}_1}}{4\pi}\,\Big|\,I^{L}(\hat{\boldsymbol{n}}_1,\hat{\boldsymbol{n}}_2)\,\Big|^2. \tag{15}$$

Note that it is essential to average the *squared* quantity over the directions. The direction average of $I^{L}(\hat{\boldsymbol{n}}_1,\hat{\boldsymbol{n}}_2)$ itself is proportional to $\delta_{L0}$, by the orthogonality of the BipoSH basis, and would therefore retain only the isotropic contribution.

These rotational and spatial averages are fundamentally related to the BipoSH formalism as we will see. The direction-averaged measure $\kappa^{L}$ takes the form in the harmonic space

$$\kappa^{L}=\frac{1}{(4\pi)^2(2L+1)^2}\sum_{M=-L}^{L}\sum_{\ell_1\ell_2}\Big|\,A^{LM}_{\ell_1\ell_2}\,\Big|^2. \tag{16}$$

The quantity $\kappa^{L}$ can be identified as the bipolar power spectrum (BiPS) introduced in A. Hajian & T. Souradeep (2003, 2005). However, the present definition incorporates normalization for both the directional and rotational averages, which accounts for the extra prefactor appearing in our expression.

As the character function is the trace of the Wigner matrix, the azimuthal index $M$ is traced over in the above expressions. Consequently, the choice of this weight function averages out the spatial orientation of the multipole.

#### 3.1.3. Diagonal Elements of Wigner Matrices as Weight

The discussion above informs us that if we use the diagonal part of the Wigner matrices $D^{L}_{MM}$ as the weight function in the rotational average, then the *orientation dependence of the anisotropies* is retained, i.e.,

$$I^{L}_{M}(\hat{\boldsymbol{n}}_1,\hat{\boldsymbol{n}}_2)=\int d\mu(\mathrm{R})D^{L*}_{MM}(\mathrm{R})\,C(\mathrm{R}\hat{\boldsymbol{n}}_1,\mathrm{R}\hat{\boldsymbol{n}}_2). \tag{17}$$

These rotational averages $I^{L}_{M}(\hat{\boldsymbol{n}}_1,\hat{\boldsymbol{n}}_2)$ are sensitive to the azimuthal index $M$. These relate to the BipoSH coefficients as

$$I^{L}_{M}(\hat{\boldsymbol{n}}_1,\hat{\boldsymbol{n}}_2)=\frac{1}{2L+1}\sum_{\ell_1\ell_2}A^{LM}_{\ell_1\ell_2}\mathbb{Y}^{LM}_{\ell_1\ell_2}(\hat{\boldsymbol{n}}_1,\hat{\boldsymbol{n}}_2). \tag{18}$$

Hence $I^{L}=\sum_{M}I^{L}_{M}$, i.e., in contrast to the character weight, using the diagonal Wigner matrices retains the azimuthal dependence by skipping the sum over azimuthal indices.

Let us now explicitly see the behavior of $I^{L}_{M}$ under SI. For an SI field, the two-point correlation function is invariant, $C(\mathrm{R}\hat{\boldsymbol{n}}_1,\mathrm{R}\hat{\boldsymbol{n}}_2)=C(\hat{\boldsymbol{n}}_1,\hat{\boldsymbol{n}}_2)$ for every $\mathrm{R}\in SO(3)$, so it factors out of the integrand in Equation (17) and

$$\begin{aligned}I^{L}_{M}(\hat{\boldsymbol{n}}_1,\hat{\boldsymbol{n}}_2)&=C(\hat{\boldsymbol{n}}_1,\hat{\boldsymbol{n}}_2)\int\mathrm{d}\mu(\mathrm{R})\,D^{L*}_{MM}(\mathrm{R})\\&=C(\hat{\boldsymbol{n}}_1,\hat{\boldsymbol{n}}_2)\,\delta_{L0}\,\delta_{M0},\end{aligned} \tag{19}$$

where we have used $D^{0}_{00}(\mathrm{R})=1$ together with the orthogonality relation Equation (7).

The same conclusion follows in the harmonic route: SI fixes the harmonic two-point function to $\langle a_{\ell_1 m_1}a_{\ell_2 m_2}\rangle=(-1)^{m_1}C_{\ell_1}\delta_{\ell_1\ell_2}\delta_{m_1-m_2}$, so that the BipoSH coefficients reduce to

$$A^{LM}_{\ell_1\ell_2}=(-1)^{\ell_1}\sqrt{2\ell_1+1}\;C_{\ell_1}\,\delta_{\ell_1\ell_2}\,\delta_{L0}\,\delta_{M0}, \tag{20}$$

and, substituting in Equation (18)

$$I^{L}_{M}(\hat{\boldsymbol{n}}_1,\hat{\boldsymbol{n}}_2)=\delta_{L0}\,\delta_{M0}\sum_{\ell}\frac{2\ell+1}{4\pi}C_{\ell}\,P_{\ell}(\hat{\boldsymbol{n}}_1\cdot\hat{\boldsymbol{n}}_2). \tag{21}$$

The surviving $L=0$ component is thus the isotropic angular correlation function itself, consistent with Equation (19). Note that Equation (21) is equivalent to performing the rotational average with uniform weight (Equation (12)), and this connection is straightforward—the uniform weight average retains only the $SO(3)$ invariant component of the two-point function. A signal at $L>0$ in $I^{L}_{M}$ is thus a signature of SI violation in the two-point function.

Two points are worth emphasizing here. The first is what $I^{L}_{M}$ at $L>0$ actually probes. For a Gaussian field, the two-point function provides a complete statistical description, so the vanishing of $I^{L}_{M}$ for all $L>0$ is equivalent to the field being SI. For a non-Gaussian field, $I^{L}_{M}$ tests only the two-point function; the three- and higher-point functions may independently violate rotational invariance, so the field may still be nSI even when its two-point function is isotropic (refer to the Appendix).

Second, a statistical inhomogeneity of the underlying three-dimensional perturbations will generically appear as an anisotropy to an off-center observer. The rotational averages test the observed sky for departures from SI. Since the CMB temperature is a field on $S^2$, a statistic constructed from $\Delta T(\hat{\boldsymbol{n}})$ alone cannot discern the origin of such departures, which may

arise from either statistical inhomogeneity or nSI in the underlying three-dimensional primordial perturbations.

Similar to the case of the character weight, one can further take the direction averages of the quantity $|I_M^L(\hat{\boldsymbol{n}}_1, \hat{\boldsymbol{n}}_2)|^2$ to arrive at a positive definite global measure of nSI components of $C(\hat{\boldsymbol{n}}_1, \hat{\boldsymbol{n}}_2)$

$$\kappa_M^L \equiv \int \frac{\mathrm{d}\Omega_{\hat{\boldsymbol{n}}_2}}{4\pi} \int \frac{\mathrm{d}\Omega_{\hat{\boldsymbol{n}}_1}}{4\pi} \left| I_M^L(\hat{\boldsymbol{n}}_1, \hat{\boldsymbol{n}}_2) \right|^2. \tag{22}$$

In the harmonic space, this measure takes the form

$$\kappa_M^L = \frac{1}{(4\pi)^2(2L+1)^2} \sum_{\ell_1\ell_2} \left| A_{\ell_1\ell_2}^{LM} \right|^2, \tag{23}$$

Interestingly, if we project the rotational average $I_M^L(\hat{\boldsymbol{n}}_1, \hat{\boldsymbol{n}}_2)$ on the BipoSH basis, we recover the BipoSH coefficients

$$A_{\ell_1\ell_2}^{LM} = (2L+1) \times \int \mathrm{d}\Omega_{\hat{\boldsymbol{n}}_1} \int \mathrm{d}\Omega_{\hat{\boldsymbol{n}}_2} \quad I_M^L(\hat{\boldsymbol{n}}_1, \hat{\boldsymbol{n}}_2) \mathbb{Y}_{\ell_1\ell_2}^{LM*}(\hat{\boldsymbol{n}}_1, \hat{\boldsymbol{n}}_2). \tag{24}$$

Summing over the internal ranks in the above expression, one can represent the reduced BipoSH coefficients (introduced in A. Hajian & T. Souradeep 2006) in terms of the rotational averages

$$A^{LM} = \sum_{\ell_1\ell_2} A_{\ell_1\ell_2}^{LM} = (2L+1) \times \int \mathrm{d}\Omega_{\hat{\boldsymbol{n}}_1} \int \mathrm{d}\Omega_{\hat{\boldsymbol{n}}_2} I_M^L(\hat{\boldsymbol{n}}_1, \hat{\boldsymbol{n}}_2) \sum_{\ell_1\ell_2} \mathbb{Y}_{\ell_1\ell_2}^{LM*}(\hat{\boldsymbol{n}}_1, \hat{\boldsymbol{n}}_2). \tag{25}$$

In the next section, we present an example to demonstrate explicitly that a nonvanishing weighted rotational average of the correlation function indicates the presence of an anisotropic signal.

## 4. Illustrative Example

We consider the phenomenological model of dipole modulation, widely adopted in the Planck analyses (Planck Collaboration 2014; Planck Collaboration 2016; Planck Collaboration 2018) to characterize the cosmic hemispherical asymmetry (S. Shaikh et al. 2019) observed in CMB

$$\Delta T(\hat{\boldsymbol{n}}) = \Delta T_{\rm iso}(\hat{\boldsymbol{n}})[1 + \epsilon(\hat{\boldsymbol{n}} \cdot \hat{\boldsymbol{p}})], \tag{26}$$

where $\hat{\boldsymbol{p}}$ defines a special direction on the sky and $\epsilon$ is a smallness parameter. The real-space angular correlation function takes the form

$$C(\hat{\boldsymbol{n}}_1, \hat{\boldsymbol{n}}_2) = C_{\rm iso}(\hat{\boldsymbol{n}}_1 \cdot \hat{\boldsymbol{n}}_2)[1 + \epsilon(\hat{\boldsymbol{n}}_1 \cdot \hat{\boldsymbol{p}} + \hat{\boldsymbol{n}}_2 \cdot \hat{\boldsymbol{p}}) + \epsilon^2(\hat{\boldsymbol{n}}_1 \cdot \hat{\boldsymbol{p}})(\hat{\boldsymbol{n}}_2 \cdot \hat{\boldsymbol{p}})]. \tag{27}$$

The leading term $C_{\rm iso}$ is the isotropic background. The $\mathcal{O}(\epsilon)$ terms represent a dipolar modulation along the special direction. The subdominant $\mathcal{O}(\epsilon^2)$ term captures the dipole–dipole correlation inducing a quadrupole-like modulation.

As the isotropic factor $C_{\rm iso}$ remains untouched by the $SO(3)$ integration Equation (17), the rotational averages are significantly simpler to compute than their harmonic counterparts $A_{\ell_1\ell_2}^{LM}$. These quantities take the following forms for the present example:

$$I_M^L(\hat{\boldsymbol{n}}_1, \hat{\boldsymbol{n}}_2) = C_{\rm iso}(\hat{\boldsymbol{n}}_1 \cdot \hat{\boldsymbol{n}}_2)\{\delta_{L0}\delta_{M0} + \epsilon\delta_{L1}\frac{4\pi}{9} Y_{1M}^*(\hat{\boldsymbol{p}})\left[Y_{1M}(\hat{\boldsymbol{n}}_1) + Y_{1M}(\hat{\boldsymbol{n}}_2)\right] + \epsilon^2 \frac{8\pi^{3/2}}{3(2L+1)^{3/2}} \mathcal{C}_{1010}^{L0} Y_{LM}^*(\hat{\boldsymbol{p}}) \times \mathbb{Y}_{11}^{LM}(\hat{\boldsymbol{n}}_1, \hat{\boldsymbol{n}}_2)\Big\}. \tag{28}$$

$I_M^L(\hat{\boldsymbol{n}}_1, \hat{\boldsymbol{n}}_2)$ extracts the multipole structure of the correlation function, explicitly mapping how the special direction $\hat{\boldsymbol{p}}$ couples to the line-of-sight directions $(\hat{\boldsymbol{n}}_1, \hat{\boldsymbol{n}}_2)$ to generate the nSI features. The monopole $(I_0^0)$ captures the dominant rotationally invariant background; it also gets an $\mathcal{O}(\epsilon^2)$ contribution from the modulation factor. The dipole $(I_M^1)$ arises at $\mathcal{O}(\epsilon)$, linearly coupling the special direction to each line of sight independently. For the $\mathcal{O}(\epsilon^2)$ term, the Clebsch–Gordan coefficient $\mathcal{C}_{1010}^{L0}$ restricts the contributions to the $L=0$ and $L=2$ sectors. The $\mathcal{O}(\epsilon^2)$ quadrupole $(I_M^2)$ contribution comes from the dipole–dipole cross correlation, characterized by the coupling of the BipoSH basis $\mathbb{Y}_{11}^{2M}(\hat{\boldsymbol{n}}_1, \hat{\boldsymbol{n}}_2)$ with the special direction.

The geometric clarity of the forms of $I_M^L$ are especially evident when compared to the BipoSH coefficients

$$A_{\ell_1\ell_2}^{LM} = (-1)^{\ell_1}\sqrt{2\ell_1+1}\, C_{\ell_1}\delta_{\ell_1\ell_2}\delta_{L0}\delta_{M0} + \epsilon\delta_{L1}\frac{2\sqrt{\pi}}{3} Y_{1M}^*(\hat{\boldsymbol{p}}) \sqrt{\frac{(2\ell_1+1)(2\ell_2+1)}{3}} \times \mathcal{C}_{\ell_1 0 \ell_2 0}^{10}\left(C_{\ell_1} + C_{\ell_2}\right) + \epsilon^2 \sqrt{\frac{4\pi}{2L+1}}\, \mathcal{C}_{1010}^{L0} Y_{LM}^*(\hat{\boldsymbol{p}}) \times \sum_{\ell}(2\ell+1)C_\ell(-1)^{\ell_1-1} \begin{Bmatrix} \ell_1 & \ell_2 & L \\ 1 & 1 & \ell \end{Bmatrix} \mathcal{C}_{\ell 010}^{\ell_1 0} \mathcal{C}_{\ell 010}^{\ell_2 0}. \tag{29}$$

Although rotational averages fully encode the breaking of rotational symmetries, their explicit line-of-sight dependence may make them challenging to analyze and represent in the context of complex phenomenological models or real CMB data. Instead, the quantity $\kappa_M^L$ provides a more practical measure: it averages out the explicit line-of-sight dependence, but still retains information of the orientation of the special direction through its azimuthal index $M$. For the present model, these are

$$\kappa_0^0 = \frac{1}{(4\pi)^2} \sum_{\ell} \left[(2\ell+1)C_\ell^2 + \frac{4\epsilon^2}{3}(\ell+1)C_\ell C_{\ell+1}\right], \tag{30}$$

$$\kappa_M^1 = \frac{\epsilon^2}{162\pi} |Y_{1M}(\hat{\boldsymbol{p}})|^2 \sum_{\ell}(\ell+1)(C_\ell + C_{\ell+1})^2, \tag{31}$$

$$\kappa_M^2 = \mathcal{O}(\epsilon^4). \tag{32}$$

The dominant contribution to the monopole $\kappa_0^0$ stems from the rotationally invariant unmodulated background. The monopole

also receives a positive $\mathcal{O}(\epsilon^2)$ shift from the modulation factor. Because the monopole lacks azimuthal dependence, this shift is independent of the orientation of the special direction. Crucially, *the dipole contribution* $\kappa^1_M \propto \epsilon^2 |Y_{1M}(\hat{\boldsymbol{p}})|^2$ *probes the geometry of the special direction*. For example, a dominant $M = 0$ projection implies the special axis is aligned with the $z$-axis of the coordinate system, while dominant $M = \pm 1$ projections imply that the special direction lies in the equatorial plane. Finally, the quadrupole power $\kappa^2_M$ gets its leading contribution of order $\mathcal{O}(\epsilon^4)$ through the dipole–dipole interaction term.

## 5. Numerical Implementation

To establish the implementability of nSI measurements in the real-space approach, we numerically compute the quantities in Equations (17) and (23) and compare them with the traditional harmonic space results. To compute $I^L_M(\hat{\boldsymbol{n}}_1, \hat{\boldsymbol{n}}_2)$ numerically, we define its estimator as

$$\tilde{I}^L_M(\hat{\boldsymbol{n}}_1, \hat{\boldsymbol{n}}_2) = \frac{1}{N_R}\sum_i^{N_R} D^{L*}_{MM}(\mathrm{R}_i)\Delta T(\mathrm{R}_i\hat{\boldsymbol{n}}_1)\Delta T(\mathrm{R}_i\hat{\boldsymbol{n}}_2), \quad (33)$$

where $N_R$ is the number of rotations sampled. The sampling in the above equation is to be performed with respect to the Haar measure on $SO(3)$. To achieve this, we use the fact that $SU(2)$ is the double cover of $SO(3)$. Since the group of unit quaternions is isomorphic to $SU(2)$, we uniformly generate unit quaternions using Shoemake's formula (K. Shoemake 1992). Shoemake's formula parametrizes the three-sphere $S^3$—which is the group manifold of $SU(2)$—using two angular variables and one radial parameter, effectively viewing the three-sphere as two coupled circles. This then reduces the problem to uniformly sampling points on these coupled circles, with the coordinates of the points forming the components of the unit quaternion ($q$). Finally, the unit quaternion is mapped to the corresponding rotation in $SO(3)$, with both $q$ and $-q$ identifying the same rotation. Further discussions on sampling on $SO(3)$ can be found in K. Shoemake (1992).

We use the `HEALPix`[3] package (K. M. Górski et al. 2005) for map computations and visualizations. Figures 1 and 2 show the ensemble averaged estimates of $\tilde{I}^1_M(\hat{\boldsymbol{n}}_1, \hat{\boldsymbol{n}}_2)$ and $\tilde{I}^0(\theta)$ (Equation (33)) for the dipole modulation model. In Figure 1, one line-of-sight direction ($\hat{\boldsymbol{n}}^*_1$) is fixed over all realizations. It can be seen that the map of $\langle \tilde{I}^1_0(\hat{\boldsymbol{n}}^*_1, \hat{\boldsymbol{n}}_2)\rangle$ closely matches the theoretical result. Figure 2 shows that the real-space estimator retrieves the isotropic component of the two-point function, while the variance of the estimator closely tracks the analytical cosmic variance.

Similarly, the estimator for $\kappa^L_M$ can be expressed as

$$\tilde{\kappa}^L_M = \frac{1}{n_p}\sum_i^{n_p} \tilde{I}^L_M[(\hat{\boldsymbol{n}}_1, \hat{\boldsymbol{n}}_2)_i]\tilde{I}^{L*}_M[(\hat{\boldsymbol{n}}_1, \hat{\boldsymbol{n}}_2)_i]. \quad (34)$$

The estimator in Equation (34) is computed by uniformly sampling the sphere and obtaining $n_p$ pairs of line-of-sight points.

[3] https://healpix.sourceforge.io

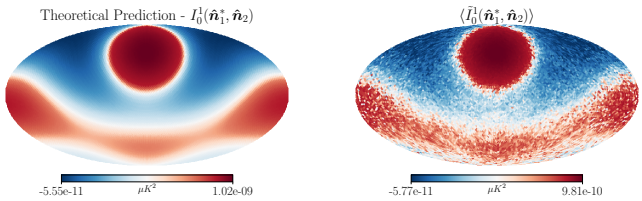



**Figure 1.** Left: theoretical prediction of $I^1_0(\hat{\boldsymbol{n}}^*_1, \hat{\boldsymbol{n}}_2)$ plotted for a dipole modulation map (`nside` = 32) with axis $\hat{\boldsymbol{p}} = \hat{\boldsymbol{n}}_z$ and modulation amplitude $\epsilon = 0.5$ (see Equation (28)). $\hat{\boldsymbol{n}}^*_1$ indicates a fixed line-of-sight direction, in this case, $\hat{\boldsymbol{n}}^*_1(\theta, \phi) = (\pi/4, 0)$. Right: ensemble averaged I˜01(n^1*,n^2) over 100 realizations with the same dipole modulation parameters.

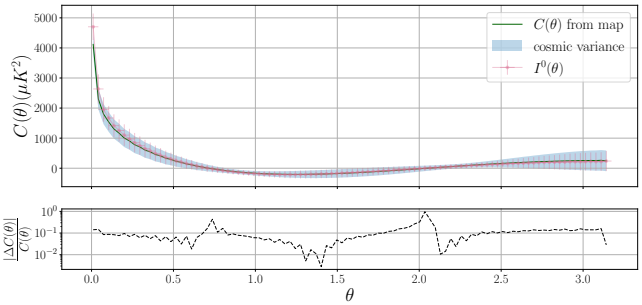



**Figure 2.** Top panel: the SI component of the two-point correlation function estimated using $\chi^L$ weighted rotational average (see Equation (14)) over 1000 realizations of a dipole modulated map (`nside` = 32) with $\epsilon = 0.5$. The markers indicate the mean of the 100 bins considered, and horizontal and vertical error bars indicate the bin width and the variance of the estimator $\tilde{I}^0$, respectively. The shaded region is the analytical cosmic variance, while the solid line is the theoretical $C(\theta)$. Bottom panel: the fractional difference between the estimated two-point correlation function and the theoretical $C(\theta)$. The two peaks observed in the fractional difference are artifacts of the zero crossing of $C(\theta)$.

Note that while the estimator $\tilde{I}^L_M(\hat{\boldsymbol{n}}_1, \hat{\boldsymbol{n}}_2)$ is unbiased, the estimator $\tilde{\kappa}^L_M$ carries a bias $B^L_M = \langle \tilde{\kappa}^L_M\rangle - \kappa^L_M$, owing to its nonlinear dependence on $\tilde{I}^L_M(\hat{\boldsymbol{n}}_1, \hat{\boldsymbol{n}}_2)$. In the harmonic space it takes the form

$$\begin{aligned} B^L_M = &\frac{1}{(4\pi)^2(2L+1)^2}\sum_{\ell_1\ell_2}\sum_{m_1m_2m_1'm_2'} \\ &\times \mathcal{C}^{LM}_{\ell_1m_1\ell_2m_2}\,\mathcal{C}^{LM}_{\ell_1m_1'\ell_2m_2'} \\ &\times \Big[\left\langle a_{\ell_1m_1}a_{\ell_2m_2}a^*_{\ell_1m_1'}a^*_{\ell_2m_2'}\right\rangle \\ &- \langle a_{\ell_1m_1}a_{\ell_2m_2}\rangle\left\langle a^*_{\ell_1m_1'}a^*_{\ell_2m_2'}\right\rangle\Big], \end{aligned} \quad (35)$$

The bias contains the four-point functions and pairs of two-point functions. Even for an SI, the Gaussian sky, $B^L_M$ at $L \neq 0$, is nonvanishing due to the residual contribution from the four-point function that survives subtraction of the second term. Consequently, a nonzero $\tilde{\kappa}^L_M$ at $L \neq 0$ is not by itself evidence of broken isotropy, and must be assessed against the expected bias. This is a caveat of the quadratic nature of $\kappa^L_M$, in contrast, the rotational average estimator $\tilde{I}^L_M$ is unbiased and hence free of such a caveat.

As the bias $B^L_M$ depends on both nSI and non-Gaussian features of the field, computing it in general requires modeling these features. However, under the assumption of Gaussianity and SI, the bias and can be obtained analytically

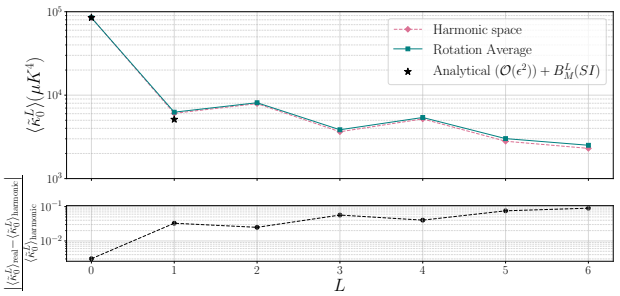



**Figure 3.** Top panel: $\langle \tilde{\kappa}_0^L \rangle$ from rotational averages (solid green line) and the corresponding harmonic space estimator (dashed red line), ensemble averaged over 1000 realizations of the dipole modulated map (nside = 32) with amplitude $\epsilon = 0.5$ and axis $\hat{\boldsymbol{p}} = \hat{\boldsymbol{n}}_z$. The black markers indicate the analytically computed $\kappa_0^L$ up to $\mathcal{O}(\epsilon^2)$ for $L \leqslant 1$ with the SI component of the bias added. Bottom panel: the fractional difference between the real and harmonic space estimators. The number of rotations sampled are of the order of $10^5$ for 5000 line-of-sight pairs.

(A. Hajian & T. Souradeep (2003)) as

$$B_M^L = \frac{1}{(4\pi)^2(2L+1)^2}\left[\sum_{\ell_1}\sum_{\ell_2=|L-\ell_1|}^{L+\ell_1} C_{\ell_1}C_{\ell_2} + \sum_{\ell_1}\sum_{\ell_2=|L-\ell_1|}^{L+\ell_1}(-1)^L C_{\ell_1}C_{\ell_2}\delta_{\ell_1\ell_2}\right]. \quad (36)$$

In Figure 3, we compare the estimators for $\tilde{\kappa}_0^L$ computed from rotational averages and harmonic space, along with theoretical estimations, evaluated up to $\mathcal{O}(\epsilon^2)$ for $L \leqslant 1$.

To ensure a better comparison, we have added the analytical Gaussian and SI bias of Equation (36) to the theoretical estimations (see A. Hajian & T. Souradeep 2003 for further details on the bias).

Importantly, the real and harmonic space results are in agreement up to a fractional deviation of $\leqslant 10^{-1}$ for low multipoles $L \leqslant 6$. Note that the bias-added theoretical prediction (Equation (30)) falls below both the real and harmonic space estimators, particularly at the $L = 1$ scale. This discrepancy can be attributed to contributions from the $\mathcal{O}(\epsilon^3)$ terms, as well as the nSI component of the bias, which are not taken into account.

We further note that the fractional difference between the real and harmonic space results grow with increasing $L$. This deviation stems from the limitation of discretely sampling the rotation group. The functional behavior of the $SO(3)$ integrand (Equation (14)) is dictated by the Wigner matrices; specifically, the character function of rotation is proportional to $\sin(\omega(L + 1/2))$, where $\omega$ is the rotation angle (D. A. Varshalovich et al. 1988). As a result, the integrand becomes highly oscillatory at higher multipoles. Consequently, for a fixed number of sampled rotations, the discrete integration becomes less accurate at higher multipoles. Such sampling errors might be rectified, keeping the computation cost in mind, by suitable scaling the number of samples with $L$.

## 6. Discussion

The real-space formalism shows promising agreement to the harmonic space counterpart, up to $\mathcal{O}(10^{-1})$ fractional deviation in the measure $\kappa_M^L$, which can be further improved with appropriate scaling of the number of rotations sampled at higher $L$.

Apart from being an alternative route to extract nSI signatures, the real-space construction is also a promising route to mitigate the nontrivial partial sky effects such as mode coupling and leakage between different polarization modes (see, e.g., E. Hivon et al. 2002; A. Lewis et al. 2002) that arise in the harmonic space decomposition. A partial sky analysis will be pursued in future work.

The rotational averages extend to higher-order correlation functions. We have shown this explicitly for the three-point correlation function (Appendix), which can be induced if the field is non-Gaussian. If the three-point function is SI, $I_M^{(3)L}$ is supported entirely at $L = 0$, regardless of the shape and amplitude of the bispectrum; for a zero-mean Gaussian field, $I_M^{(3)L}$ vanishes identically for every $L$, including $L = 0$.

Similarly this framework can be used to study the weak gravitational lensing of the CMB (C. S. Carvalho & K. Moodley 2010; M. Bucher et al. 2012) and can also be generalized to higher spin fields such as CMB polarization. Since this framework is explicitly rooted in symmetry, it can be used to study phenomena with known breakdowns of rotational symmetry, for example, in models of nontrivial topologies (M. Lachieze-Rey & J.-P. Luminet 1995; A. Hajian & T. Souradeep 2003; J. R. Bond et al. 1998). Furthermore, this geometric framework can be extended to study isotropy violations across a broader class of fields including astrophysics, nuclear physics (J. L. Friar et al. 1981; S. N. Ershov 2004), and atomic and molecular physics (N. L. Manakov et al. 2002; A. V. Meremianin 2005).

## Acknowledgments

The authors acknowledge the HPC facilities at RRI. V.R. thanks Rishav Saha for useful discussions. D.M. thanks Harkirat Singh Sahota for valuable comments and suggestions. D.M. thanks Raman Research Institute for support through postdoctoral fellowship. T.S. acknowledges support from the J. C. Bose Grant of Anusandhan National Research Foundation, India.

## Appendix
## Rotational Averages of CMB Three-point Correlation Function

The rotational average formalism can be extended to N-point function as

$$I_M^{(N)L}(\hat{\boldsymbol{n}}_1, \hat{\boldsymbol{n}}_2, \ldots, \hat{\boldsymbol{n}}_N) = \int \mathrm{d}\mu(\mathrm{R})\, D_{MM}^{L*}(\mathrm{R}) \times \mathcal{N}(\mathrm{R}\hat{\boldsymbol{n}}_1, \mathrm{R}\hat{\boldsymbol{n}}_2, \ldots, \mathrm{R}\hat{\boldsymbol{n}}_N), \quad (A1)$$

with $\mathcal{N}(R\hat{\boldsymbol{n}}_1, R\hat{\boldsymbol{n}}_2, \ldots, R\hat{\boldsymbol{n}}_N) = \langle \Delta T(\hat{\boldsymbol{n}}_1)\Delta T(\hat{\boldsymbol{n}}_2)\ldots\Delta T(\hat{\boldsymbol{n}}_N)\rangle$, a real function defined on $\underbrace{S^2 \times S^2 \times \cdots \times S^2}_{N \text{ times}}$.

We focus specifically on the three-point function here. We denote the three-point function as $\mathcal{T}(\hat{\boldsymbol{n}}_1, \hat{\boldsymbol{n}}_2, \hat{\boldsymbol{n}}_3) = \langle \Delta T(\hat{\boldsymbol{n}}_1)\Delta T(\hat{\boldsymbol{n}}_2)\Delta T(\hat{\boldsymbol{n}}_3)\rangle$, a real function defined on $S^2 \times S^2 \times S^2$. The harmonic representation of a three-point function is provided by the tripolar spherical harmonic (TripoSH) basis, which couples the three internal ranks $(\ell_1, \ell_2, \ell_3)$ corresponding to the three directions $(\hat{\boldsymbol{n}}_1, \hat{\boldsymbol{n}}_2, \hat{\boldsymbol{n}}_3)$ into a state of total angular momentum $L$ through an

intermediate rank $\ell_{23}$ (D. A. Varshalovich et al. 1988)

$$\begin{aligned}\mathbb{T}^{LM}_{\ell_1\ell_2\ell_3\ell_{23}}(\hat{\boldsymbol{n}}_1, \hat{\boldsymbol{n}}_2, \hat{\boldsymbol{n}}_3) &\equiv \{Y_{\ell_1}(\hat{\boldsymbol{n}}_1) \otimes \{Y_{\ell_2}(\hat{\boldsymbol{n}}_2) \otimes Y_{\ell_3}(\hat{\boldsymbol{n}}_3)\}_{\ell_{23}}\}_{LM} \\ &= \sum_{m_1m_2m_3m_{23}} \mathcal{C}^{LM}_{\ell_1m_1\ell_{23}m_{23}}\, \mathcal{C}^{\ell_{23}m_{23}}_{\ell_2m_2\ell_3m_3}\, Y_{\ell_1m_1}(\hat{\boldsymbol{n}}_1) \\ &\quad \times Y_{\ell_2m_2}(\hat{\boldsymbol{n}}_2)\, Y_{\ell_3m_3}(\hat{\boldsymbol{n}}_3),\end{aligned} \tag{A2}$$

where the triangle inequalities $|\ell_2 - \ell_3| \leqslant \ell_{23} \leqslant \ell_2 + \ell_3$ and $|\ell_1 - \ell_{23}| \leqslant L \leqslant \ell_1 + \ell_{23}$, together with the azimuthal conditions $m_{23} = m_2 + m_3$ and $M = m_1 + m_2 + m_3$, are assumed. The three-point function is then expanded as

$$\mathcal{T}(\hat{\boldsymbol{n}}_1, \hat{\boldsymbol{n}}_2, \hat{\boldsymbol{n}}_3) = \sum_{LM} \sum_{\ell_1\ell_2\ell_3\ell_{23}} t^{LM}_{\ell_1\ell_2\ell_3\ell_{23}}\, \mathbb{T}^{LM}_{\ell_1\ell_2\ell_3\ell_{23}}(\hat{\boldsymbol{n}}_1, \hat{\boldsymbol{n}}_2, \hat{\boldsymbol{n}}_3), \tag{A3}$$

where $t^{LM}_{\ell_1\ell_2\ell_3\ell_{23}}$ are the TripoSH coefficients.

The essential property for our purpose is that the TripoSH basis, like the BipoSH basis, transforms under a rotation $\mathrm{R} \in SO(3)$ analogously to Equation (6) (D. A. Varshalovich et al. 1988)

$$\begin{aligned}&\mathbb{T}^{LM}_{\ell_1\ell_2\ell_3\ell_{23}}(\mathrm{R}\hat{\boldsymbol{n}}_1, \mathrm{R}\hat{\boldsymbol{n}}_2, \mathrm{R}\hat{\boldsymbol{n}}_3) \\ &= \sum_{M'} D^{L}_{M'M}(\mathrm{R})\, \mathbb{T}^{LM'}_{\ell_1\ell_2\ell_3\ell_{23}}(\hat{\boldsymbol{n}}_1, \hat{\boldsymbol{n}}_2, \hat{\boldsymbol{n}}_3).\end{aligned} \tag{A4}$$

A rotation via the Wigner-$D$ matrix thus mixes only the azimuthal index $M$, leaving the total rank $L$ and the internal ranks $\ell_1$, $\ell_2$, $\ell_3$, $\ell_{23}$ untouched. Adopting the diagonal Wigner elements as the weight, as in Section 3.1.3, the rotational average of the three-point function is

$$I^{(3)L}_{M}(\hat{\boldsymbol{n}}_1, \hat{\boldsymbol{n}}_2, \hat{\boldsymbol{n}}_3) = \int \mathrm{d}\mu(\mathrm{R})\, D^{L*}_{MM}(\mathrm{R})\, \mathcal{T}(\mathrm{R}\hat{\boldsymbol{n}}_1, \mathrm{R}\hat{\boldsymbol{n}}_2, \mathrm{R}\hat{\boldsymbol{n}}_3), \tag{A5}$$

and substituting Equations (A3) and (A4) into the above definition, one obtains

$$\begin{aligned}&I^{(3)L}_{M}(\hat{\boldsymbol{n}}_1, \hat{\boldsymbol{n}}_2, \hat{\boldsymbol{n}}_3) \\ &= \frac{1}{2L+1} \sum_{\ell_1\ell_2\ell_3\ell_{23}} t^{LM}_{\ell_1\ell_2\ell_3\ell_{23}}\, \mathbb{T}^{LM}_{\ell_1\ell_2\ell_3\ell_{23}}(\hat{\boldsymbol{n}}_1, \hat{\boldsymbol{n}}_2, \hat{\boldsymbol{n}}_3).\end{aligned} \tag{A6}$$

This is the three-point analog of Equation (18): the indices ($L$, $M$) carried by $I^{(3)L}_{M}$ are the total angular momentum and azimuthal index of the TripoSH expansion, summed over all internal ranks. As in the two-point case, this is what makes the rotational average economical: $I^{(3)L}_{M}$ is obtained directly as an average over rotated configurations, without having to evaluate the individual TripoSH coefficients $t^{LM}_{\ell_1\ell_2\ell_3\ell_{23}}$, whose internal rank coupling is considerably more involved than in the two-point case.

The behavior of this rotation average for a statistically isotropic field is straightforward to obtain. Under SI, by definition, the three-point function is invariant, $\mathcal{T}(\mathrm{R}\hat{\boldsymbol{n}}_1, \mathrm{R}\hat{\boldsymbol{n}}_2, \mathrm{R}\hat{\boldsymbol{n}}_3) = \mathcal{T}(\hat{\boldsymbol{n}}_1, \hat{\boldsymbol{n}}_2, \hat{\boldsymbol{n}}_3)$ for every $\mathrm{R} \in SO(3)$, so it factors out of the integrand in Equation (A5) and

$$\begin{aligned}I^{(3)L}_{M}(\hat{\boldsymbol{n}}_1, \hat{\boldsymbol{n}}_2, \hat{\boldsymbol{n}}_3) &= \mathcal{T}(\hat{\boldsymbol{n}}_1, \hat{\boldsymbol{n}}_2, \hat{\boldsymbol{n}}_3) \int \mathrm{d}\mu(\mathrm{R})\, D^{L*}_{MM}(\mathrm{R}) \\ &= \mathcal{T}(\hat{\boldsymbol{n}}_1, \hat{\boldsymbol{n}}_2, \hat{\boldsymbol{n}}_3)\, \delta_{L0}\, \delta_{M0},\end{aligned} \tag{A7}$$

where we have used $D^{0}_{00}(\mathrm{R}) = 1$ and the orthogonality relation Equation (7).

This result can also be corroborated in harmonic space, where SI restricts the TripoSH spectrum to a single nonvanishing component, $L = 0$, regardless of the internal coupling structure. To see this, let us note that SI fixes the harmonic three-point function to the form (D. A. Varshalovich et al. 1988)

$$\langle a_{\ell_1m_1} a_{\ell_2m_2} a_{\ell_3m_3} \rangle = B_{\ell_1\ell_2\ell_3} \begin{pmatrix} \ell_1 & \ell_2 & \ell_3 \\ m_1 & m_2 & m_3 \end{pmatrix}, \tag{A8}$$

where $B_{\ell_1\ell_2\ell_3}$ is the bispectrum that captures the couplings of the internal ranks. In terms of the spherical harmonic coefficients $a_{\ell m}$, the three-point function reads

$$\begin{aligned}\mathcal{T}(\hat{\boldsymbol{n}}_1, \hat{\boldsymbol{n}}_2, \hat{\boldsymbol{n}}_3) &= \sum_{\ell_1\ell_2\ell_3} \sum_{m_1m_2m_3} \langle a_{\ell_1m_1} a_{\ell_2m_2} a_{\ell_3m_3} \rangle \\ &\quad \times Y_{\ell_1m_1}(\hat{\boldsymbol{n}}_1)\, Y_{\ell_2m_2}(\hat{\boldsymbol{n}}_2)\, Y_{\ell_3m_3}(\hat{\boldsymbol{n}}_3).\end{aligned} \tag{A9}$$

Projecting Equation (A3) on the TripoSH basis, using Equation (A9) and the orthonormality of the spherical harmonics relates the TripoSH coefficients to the harmonic three-point function

$$\begin{aligned}t^{LM}_{\ell_1\ell_2\ell_3\ell_{23}} &= \sum_{m_1m_2m_3m_{23}} \langle a_{\ell_1m_1} a_{\ell_2m_2} a_{\ell_3m_3} \rangle \\ &\quad \times \mathcal{C}^{LM}_{\ell_1m_1\ell_{23}m_{23}}\, \mathcal{C}^{\ell_{23}m_{23}}_{\ell_2m_2\ell_3m_3},\end{aligned} \tag{A10}$$

which under SI (A8) collapses to

$$t^{LM}_{\ell_1\ell_2\ell_3\ell_{23}} = (-1)^{\ell_1+\ell_2+\ell_3} B_{\ell_1\ell_2\ell_3}\, \delta_{\ell_{23}\ell_1}\, \delta_{L0}\, \delta_{M0}. \tag{A11}$$

The key observation from the above relation is that SI populates only the $L = 0$ component of $t^{LM}_{\ell_1\ell_2\ell_3\ell_{23}}$, and thus $I^{(3)L}_{M}$ (through Equation A6), regardless of the strength or shape of the non-Gaussianity $B_{\ell_1\ell_2\ell_3}$.

Note that for a zero-mean Gaussian field the three-point function vanishes identically, and with it every $I^{(3)L}_{M}$, including the $L = 0$ mode. For a non-Gaussian field with a nonvanishing three-point function, Equation (A7) confines the signal entirely to $L = 0$ under SI, so that a signal at $L \neq 0$ implies a violation of SI in the three-point function. This is not contained in the two-point measure: for a non-Gaussian field, SI of the two-point function does not imply SI of the field, and $I^{(3)L}_{M}$ can be nonzero at $L \neq 0$ while $I^{L}_{M}$ vanishes there.

The above exercise emphasizes that the real-space approach provides a more intuitive and direct way to capture nSI features in the field compared to the harmonic space route, as it does not require computation of the TripoSH coefficients up to arbitrarily high internal ranks.

## ORCID iDs

Vaishali R https://orcid.org/0009-0004-7856-9587
Dipayan Mukherjee https://orcid.org/0000-0002-5267-1944
Akshank Tyagi https://orcid.org/0009-0002-2757-1957
Tarun Souradeep https://orcid.org/0000-0003-3764-8102

## References

Aluri, P. K., Paolo, C., Pravabati, C., et al. 2023, CQGra, 40, 094001
Bartolo, N., Dimastrogiovanni, E., Liguori, M., Matarrese, S., & Riotto, A. 2012, JCAP, 2012, 029
Bond, J. R., Pogosyan, D., & Souradeep, T. 1998, CQGra, 15, 2671
Bucher, M., Carvalho, C. S., Moodley, K., & Remazeilles, M. 2012, PhRvD, 85, 043016

Carroll, S. M., Tseng, C.-Y., & Wise, M. B. 2010, PhRvD, 81, 083501
Carvalho, C. S., & Moodley, K. 2010, PhRvD, 81, 123010
Das, S., Mitra, S., Rotti, A., Pant, N., & Souradeep, T. 2016, A&A, 591, A97
Dipanshu, Souradeep, T., & Hirve, S. 2023, ApJ, 954, 181
Ershov, S. N. 2004, PhRvC, 70, 054604
Friar, J. L., Tomusiak, E. L., Gibson, B. F., & Payne, G. L. 1981, PhRvC, 24, 677
Gordon, C. 2007, ApJ, 656, 636
Górski, K. M., Hivon, E., Banday, A. J., et al. 2005, ApJ, 622, 759
Hajian, A., & Souradeep, T. 2003, ApJL, 597, L5
Hajian, A., & Souradeep, T. 2005, arXiv:astro-ph/0501001
Hajian, A., & Souradeep, T. 2006, PhRvD, 74, 123521
Hivon, E., Gorski, K. M., Netterfield, C. B., et al. 2002, ApJ, 567, 2
Joshi, N., Jhingan, S., Souradeep, T., & Hajian, A. 2010, PhRvD, 81, 083012
Kothari, R., Ghosh, S., Rath, P. K., Kashyap, G., & Jain, P. 2016, MNRAS, 460, 1577
Kumar, S., Rotti, A., Aich, M., et al. 2015, PhRvD, 91, 043501
Lachieze-Rey, M., & Luminet, J.-P. 1995, PhR, 254, 135
Lewis, A., Challinor, A., & Turok, N. 2002, PhRvD, 65, 023505
Manakov, N. L., Meremianin, A. V., & Starace, A. F. 2002, JPhB, 35, 77
Meremianin, A. V. 2005, JPhB, 38, 757
Mitra, S., Sengupta, A. S., & Souradeep, T. 2004, PhRvD, 70, 103002
Mukherjee, S., & Souradeep, T. 2014, PhRvD, 89, 063013
Planck Collaboration 2014, A&A, 571, A23
Planck Collaboration 2016, A&A, 594, A16
Planck Collaboration 2020a, A&A, 641, A1
Planck Collaboration 2020b, A&A, 641, A7
Planck Collaboration 2018, A&A, 641, A7
Prunet, S., Uzan, J.-P., Bernardeau, F., & Brunier, T. 2005, PhRvD, 71, 083508
Ragavendra, H. V., Mukherjee, D., & Sethi, S. K. 2025, PhRvD, 111, 023541
Rath, P. K., Aluri, P. K., & Jain, P. 2015, PhRvD, 91, 023515
Schwarz, D. J., Copi, C. J., Huterer, D., & Starkman, G. D. 2016, CQGra, 33, 184001
Shaikh, S., Mukherjee, S., Das, S., Wandelt, B. D., & Souradeep, T. 2019, JCAP, 2019, 007
Shoemake, K. 1992, in Graphic Gems III, ed. D. Kirk (Academic Press), 124
Szapudi, I., Prunet, S., & Colombi, S. 2001, arXiv:astro-ph/0107383
Varshalovich, D. A., Moskalev, A. N., & Khersonskii, V. K. 1988, Quantum Theory of Angular Momentum: Irreducible Tensors, Spherical Harmonics, Vector Coupling Coefficients, 3nj Symbols (World Scientific Publishing Company)
Wu, K. K. S., Lahav, O., & Rees, M. J. 1999, Natur, 397, 225